Published online 10 June 2013 *Nucleic Acids Research, 2013, Vol. 41, No. 15* ***7485–7500***
doi:10.1093/nar/gkt490

Structure-function analysis of the 5′ end of yeast U1 snRNA highlights genetic interactions with the Msl5•Mud2 branchpoint-binding complex and other spliceosome assembly factors

Beate Schwer[1,*], Jonathan Chang[2] and Stewart Shuman[2,*]

[1]Microbiology and Immunology Department, Weill Cornell Medical College, New York, NY 10065, USA and [2]Molecular Biology Program, Sloan-Kettering Institute, New York, NY 10065, USA

Received March 28, 2013; Revised May 7, 2013; Accepted May 12, 2013

ABSTRACT

Yeast pre-mRNA splicing initiates via formation of a complex comprising U1 snRNP bound at the 5′ splice site (5′SS) and the Msl5•Mud2 heterodimer engaged at the branchpoint (BP). Here, we present a mutational analysis of the U1 snRNA, which shows that although enlarging the 5′ leader between the TMG cap and the ^{3}ACUUAC^{8} motif that anneals to the 5′SS is tolerated, there are tight constraints on the downstream spacer between ^{3}ACUUAC^{8} and helix 1 of the U1 fold. We exploit U1 alleles with 5′ extensions, variations in the ^{3}ACUUAC^{8} motif, downstream mutations and a longer helix 1 to discover new intra-snRNP synergies with U1 subunits Nam8 and Mud1 and the trimethylguanosine (TMG) cap. We describe novel mutations in U1 snRNA that bypass the essentiality of the DEAD-box protein Prp28. Structure-guided mutagenesis of Msl5 distinguished four essential amino acids that contact the BP sequence from nine other BP-binding residues that are inessential. We report new synthetic genetic interactions of the U1 snRNP with Msl5 and Mud2 and with the nuclear cap-binding subunit Cbc2. Our results fortify the idea that spliceosome assembly can occur via distinct genetically buffered microscopic pathways involving cross-intron-bridging interactions of the U1 snRNP•5′SS complex with the Mud2•Msl5•BP complex.

INTRODUCTION

The composition, function and dynamics of the pre-mRNA splicing machinery (the 'spliceosome') in the budding yeast *Saccharomyces cerevisiae* have been elucidated genetically and biochemically (1–3). The yeast spliceosome transits through assembly, activation, catalysis and disassembly steps that are programmed by the U1, U2, U4, U5 and U6 snRNPs and an army of proteins that interact with the snRNPs and the pre-mRNA. The first stage in spliceosome assembly entails the formation of a complex comprising the U1 snRNP bound at the intronic 5′ splice site (5′SS; consensus sequence: 5′-GUAUGU) and the Msl5•Mud2 protein heterodimer engaged at the intron branchpoint (BP) (consensus sequence: 5′-UACU AAC). Bridging interactions between U1 snRNP and Msl5•Mud2 serve to stabilize the complex and prepare a scaffold for recruitment of the U2 snRNP to the BP.

The yeast U1 snRNP consists of a trimethylguanosine (TMG)-capped 568-nt U1 snRNA, a toroidal Sm protein ring composed of seven subunits (present also in the U2, U4 and U5 snRNPs), and 10 additional protein subunits unique to the yeast U1 snRNP: Prp39, Prp40, Snu71, Snu56, Snp1, Mud1, Luc7, Prp42, Nam8 and Yhc1 (4–10). Yeast U1-specific subunits Snp1, Mud1 and Yhc1 are conserved in human U1 snRNP as U1-70K, U1-A and U1-C, respectively. The 5′ sequence of yeast U1 RNA—m^{2,2,7}GpppAUACUUACC—is conserved in the much smaller human U1 snRNA (164 nt) and contains a hexanucleotide motif (underlined) complementary to the consensus 5′SS. This U1 5′ sequence anneals to the pre-mRNA to nucleate an early assembly complex. The U1 snRNP protein subunits interact with U1 RNA sequences and/or secondary structures, contact the pre-mRNA or contact other protein components of the spliceosome during its initial assembly (11–13). Additional non-snRNP elements aid in U1•pre-mRNA complex assembly, including the pre-mRNA m^{7}G cap structure in association with the yeast nuclear cap-binding complex (CBC: a Sto1•Cbc2 heterodimer) (14). The U1 snRNP is ultimately displaced from the

*To whom correspondence should be addressed. Tel: +212 746 6518; Email: bschwer@med.cornell.edu
Correspondence may also be addressed to Stewart Shuman. Tel: +212 639 7145; Fax: +212 717 3623; Email: s-shuman@ski.mskcc.org

pre-mRNA•U1•U2-containing spliceosome at the point when the U5•U4•U6 tri-snRNP complex joins *en route* to forming a pre-mRNA•U2•U5•U6 spliceosome. Dissociation of U1 snRNP is thought to be triggered by the essential DEAD-box protein Prp28 (15,16), acting to disrupt the short U1:5′SS RNA duplex or remodel protein–RNA contacts at the 5′SS (or both).

Although yeast U1 RNA is essential for viability, substantial chunks of the U1 primary structure (more than half) are dispensable for cell growth (17,18). This situation inspired an elegant and highly successful genetic screen by the Rosbash laboratory for yeast mutations that caused synthetic lethality with an otherwise viable U1 snRNA mutation in which a large internal deletion was combined with a G27A change in the stem-loop-1 (SL1) sequence that interacts with U1-70K (19). The 'Mutant-U1-Die' or 'MUD' screen identified the genes encoding four of the U1-specific subunits: Mud1, Snu56/Mud10, Nam8/Mud15 and Prp42/Mud16 (5,19). The screen also identified the Cbc2/Mud13 subunit of nuclear CBC and the Mud2 subunit of the yeast BP-binding protein complex (Mud2 being the yeast homolog of mammalian U2AF65) (20,21). The findings that Mud1, Nam8, Cbc2 and Mud2 are themselves inessential for yeast vegetative growth immediately highlighted a network of genetically buffered functions centered around U1 snRNP during early spliceosome assembly. The Rosbash laboratory then bootstrapped the viable *mud2*Δ mutant to execute a 'Mud2 synthetic lethal' (MSL) screen and thereby identify Msl5, the yeast BP-binding protein, and Msl1, the U2B″ subunit of the U2 snRNP (22,23).

Additional directed and genome-wide synthetic genetic array analyses have greatly expanded the network of mutational synergies involving: the U1 snRNP subunits Mud1, Nam8, Luc7 and Yhc1; the TMG cap structure of U1 snRNA (via inactivation of TMG synthase Tgs1); m^7G cap binding by nuclear CBC; and the Msl5•Mud2 BP binding complex (24–32). Such genetic interactions among individually dispensable players (or otherwise benign mutations in essential factors) that act in a common pathway meet an operational definition of redundancy. Genetic redundancy does not necessitate that the synthetic interactor proteins or RNA elements perform the same task, but it rather suggests that spliceosome assembly can be accomplished or stabilized via different microscopic sub-pathways.

In the present study, we interrogate structure–function relations of the 5′ end of yeast U1 snRNA, by studying the effects of 5′ extensions; nucleobase changes in the ^{3}ACUUAC^8 sequence that pairs with the 5′SS; and insertions, deletions and nucleobase changes in the flanking ^{9}CUU^{11} segment that interacts with U1-C and connects the U1•5′SS RNA duplex to helix 1 of the U1 RNA fold (4,8). We find that extending the segment upstream of the ^{3}ACUUAC^8 element has no effect on growth but is synthetically lethal or sick with mutations affecting TMG capping, m^7G cap-binding by CBC, U1 snRNP protein Nam8 and the Msl5•Mud2 BP-binding complex. Insertions of 1 or 3 nt downstream of ^{3}ACUUAC^8 are viable, but display synthetic phenotypes; by contrast, insertions of ≥5 nucleotides are lethal, suggesting that the spacing between the U1•5′SS RNA duplex and helix 1 is important for U1 snRNP function. Changes that increase the length of helix 1 are benign *per se* but synthetic in combination with other agents of spliceosome assembly. Viable mutations within the ^{3}ACUUAC^8 element display allele-specific synergies. We also indentify novel mutations in U1 snRNA that bypass the essentiality of Prp28. Our results reveal a rich network of intramolecular and intermolecular genetic interactions of the yeast U1 snRNP, especially with the BP-binding protein Msl5.

MATERIALS AND METHODS

U1 expression plasmids and mutants

A 1.3-kb DNA segment bearing the *SNR19* (*U1*) gene was amplified from *S. cerevisiae* genomic DNA by PCR using a forward primer that introduced an XhoI site 550 nt upstream of the transcription start site (+1) of U1 snRNA and a reverse primer downstream of a HindIII site at position +755. The DNA fragment was inserted into centromeric plasmids pRS316 (*URA3*) and pRS415 (*LEU2*). The resulting yeast expression plasmids p316-U1 and p415-U1 include the 568-nt U1 snRNA sequence plus 550 and 187 nt of upstream and downstream sequences. Mutations (insertions, deletions and single nucleotide changes) were introduced into the U1 plasmid by two-stage PCR overlap extension with mutagenic primers. The U1 genes were sequenced completely to confirm that no unwanted changes were acquired during amplification and cloning.

Msl5 expression plasmids and mutants

CEN LEU2 plasmids bearing wild-type and mutated *MSL5* genes under the control of the native *MSL5* promoter have been described (31). New missense mutations L169A, R172A, L176A, I189A, R190A, L256A and L259A in the KH-QUA2 domain and P97A, P98A, Y100A and Y100F in the PPxY motif were introduced into *MSL5* by two-stage PCR overlap extension with mutagenic primers. The PCR products were digested and then inserted into the pRS415-based *MSL5* expression plasmid (31). The *MSL5* genes were sequenced completely to confirm that no unwanted changes were acquired during amplification and cloning. *CEN HIS3 MSL5* plasmids were constructed by subcloning 2.2-kb *MSL5* fragments (excised with XhoI and SacI from pRS415-MSL5) into pRS413.

Yeast strains and tests of U1 function *in vivo*

To develop a plasmid shuffle assay for gauging mutational effects on U1 function, we generated a *U1Δ* strain that relies for viability on maintenance of the wild-type *U1* gene on a *CEN URA3* plasmid, p316-U1. In brief, we first replaced the *U1* locus from position +1 to +532 with a *kanMX* cassette in the BY4743 diploid strain and then transformed the heterozygous diploid with p316-U1. The diploid was sporulated, asci were dissected and haploid *U1Δ* Ura$^+$ progeny were recovered. *U1Δ* (p316-U1) cells were resistant to G418 and unable to grow on

medium containing 0.75 mg/ml 5-fluoroorotic acid (FOA). To assay the function of wild-type and mutated *U1* alleles, *U1Δ* (p316-U1) cells were transfected with *CEN LEU2 U1* plasmids. Individual Leu^+ transformants were selected and streaked on agar medium containing FOA. The plates were incubated at 20, 30 or 37°C, and mutants that failed to form macroscopic colonies at any temperatures after 10 d were deemed lethal. Individual FOA-resistant colonies with viable *U1* alleles were grown to mid-log phase in yeast extract, peptone, dextrose (YPD) broth and adjusted to the same A_{600} values. Aliquots (3 µl) of serial 10-fold dilutions were spotted to YPD agar plates, which were then incubated at temperatures ranging from 18 to 37°C.

We also developed plasmid shuffle assays to test the mutational effects on U1 function in *mud2*Δ, *tgs1*Δ, *nam8*Δ, *mud1*Δ, *swt21*Δ, *brr1*Δ, *cbc2-Y24A*, *swm2*Δ and *tgs1Δ cbc2-Y24A* cells (7,27,29–32) using standard genetic manipulations of mating, sporulation and dissection. We thereby generated *mud2*Δ *U1Δ* (p316-U1), *nam8*Δ *U1Δ* (p316-U1), *mud1*Δ *U1Δ* (p316-U1), *tgs1*Δ *U1Δ* (p316-U1), *swt21*Δ *U1Δ* (p316-U1), *swm2*Δ *U1Δ* (p316-U1), *brr1*Δ *U1Δ* (p316-U1), *cbc2-Y24A U1Δ* (p316-U1) and *tgs1*Δ *cbc2-Y24A U1Δ* (p316-U1) cells, which were unable to grow on FOA-containing medium, unless they had been transformed with wild-type *U1* or a functional *U1* mutant allele on a *CEN LEU2* plasmid before FOA selection. To investigate genetic interactions of U1 mutants with the essential *MSL5* and *PRP28* genes, we first generated heterozygous *msl5*Δ/*MSL5 U1Δ*/*U1* and *prp28*Δ/*PRP28 U1Δ*/*U1* diploids by crossing *msl5Δ*::*natMX* p316-MSL5 and *prp28Δ::natMX* p316-PRP28 cells with *U1Δ::kanMX* p316-U1 cells of the opposite mating type, selecting diploids on YPD medium containing G418 and clonNat and plating them to FOA-containing medium. The heterozygous diploids were then transformed with *CEN URA3 U1 MSL5* (p316-U1-MSL5) or *CEN URA3 U1 PRP28* (p316-U1-PRP28) plasmids. [In these plasmids, the *U1* gene (−550 to +755) is arranged in a head-to-head configuration with the *MSL5* gene or the *PRP28* gene (−520 to +2120).] Ura^+ heterozygous diploids were subjected to sporulation and tetrad dissection, after which haploid *prp28*Δ *U1Δ* (p316-U1-PRP28 and *msl5*Δ *U1Δ* (p316-U1-MSL5) progeny were recovered. These cells were unable to grow on FOA medium, but the double-deletion strains could be complemented by cotransformation with p(*CEN LEU2 U1*) plus either p(*CEN HIS3 MSL5*) or p(*CEN HIS3 PRP28*).

Primer extension analysis of U1 5′ ends

U1Δ cells bearing *CEN LEU2 U1* plasmids were grown in YPD broth to mid-log phase. Cellular RNA was isolated using an RNeasy kit (Qiagen). Aliquots (20 µg of RNA) were used as templates for reverse transcriptase-catalyzed extension of 5′ ^{32}P-labeled primers 5′-d(GAATGGAAAC GTCAGCAAACAC) and 5′-d(CTTAAAAAGTCTCTT CCCGTC) that are complementary to U1 and U2 snRNA, respectively. The primer extension reactions were performed as described previously (33).

RESULTS

Effect of U1 5′ extensions that distance the cap from the ^{3}ACUUAC^8 sequence

Our interest in the 5′ end of yeast U1 snRNA was sparked by our earlier findings that (i) nuclear CBC became a stoichiometric subunit of the U1 snRNP in yeast *tgs1*Δ cells that lack the methyltransferase enzyme that converts m^7G caps to TMG caps and (ii) the cold-sensitive (*cs*) growth phenotype of yeast *tgs1*Δ cells was rescued by mutations in the cap-binding pocket of nuclear CBC that have no effect on growth *per se* (7,32). Our inference was that ectopic binding of CBC to the residual m^7G U1 snRNA cap was a key factor in the *tgs1*Δ *cs* phenotype and that reducing CBC affinity for the m^7G U1 snRNA cap restored normal growth. Because the U1 snRNA cap is located just 2 nt upstream of the ^{3}ACUUAC^8 sequence that pairs with the pre-mRNA 5′SS, we considered that steric hindrance by CBC at the U1 5′ end might interfere with U1 function, in which case increasing the physical distance between CBC and the ^{3}ACUUAC^8 sequence might suppress the *tgs1*Δ *cs* defect.

To test this idea, we extended the 5′ sequence of the *U1* gene by 5, 10, 15, 20, 25 or 30 nt, as depicted in Figure 1A. The wild-type (*WT*) and 5′-extended *U1* alleles under the control of the native *U1* promoter were placed on *CEN LEU2* plasmids and tested for function *in vivo* by plasmid shuffle in a yeast strain deleted at the chromosomal *U1* locus but bearing a *WT U1* gene on a *CEN URA3* plasmid. All of the 5′-extended *U1* alleles supported growth of yeast *U1*Δ cells on medium containing FOA, a drug that selects against the *CEN URA3 U1* plasmid. The *U1 +5*, *+10*, *+15*, *+20*, *+25* and *+30* strains grew as well as *U1 WT* cells at 20, 25, 30, 34 and 37°C, as gauged by spotting serial dilutions of the respective strains on YPD agar (Figure 1B). To assess whether the newly inserted sequences at the 5′ end of the *U1* gene were transcribed into the U1 snRNA, we performed primer extension analysis on total RNA isolated from yeast cells bearing the *WT* and 5′-extended *U1* alleles (Figure 1C). A 5′ ^{32}P-labeled DNA oligonucleotide complementary to yeast U1 snRNA was extended by reverse transcriptase to yield a discrete cDNA corresponding in size to the distance (in nucleotides) from the primer 5′ end to the 5′ end of the U1 snRNA. A second 5′ ^{32}P-labeled DNA oligonucleotide complementary to U2 snRNA was included in the reverse transcription reactions as a control. Denaturing polyacrylamide gel electrophoresis (PAGE) analysis of the primer extension products revealed that the 5′ ends of the U1 snRNAs were shifted serially 'upstream' by 5-nt intervals, as expected from the U1 DNA sequences. Thus, the DNA additions did not alter the site of transcription initiation directed by the 5′-flanking *U1* gene promoter. The amounts of U1 cDNA synthesized from total RNAs derived from the *WT* and 5′-extended *U1* yeast strains were similar, signifying that the steady-state levels of U1 snRNA were not affected by the 5′ leader sequences. The 5′ ends and steady-state levels of U2 snRNAs were unaltered by the U1 mutations.

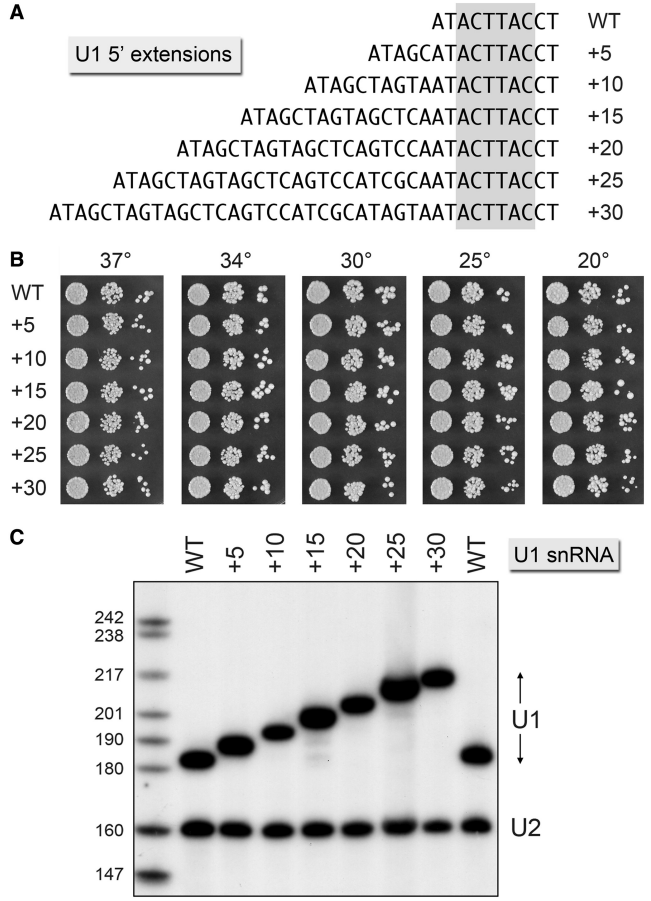

Figure 1. U1 snRNAs with extended 5′ ends are functional. (**A**) The DNA sequences are shown for the 5′ ends of wild-type U1 (WT) and the mutant variants +5, +10 and so forth, named according to the number of nucleotides inserted upstream of the ^{3}ACTTAC^{8} segment (highlighted in gray) that pairs with the intron 5′SS. (**B**) The growth phenotypes of *U1*Δ p(*CEN LEU2 U1*) cells bearing the indicated U1 alleles were assessed as follows. Liquid cultures were grown to mid-log phase at 30°C and adjusted to the same A_{600}. Aliquots (3 µl) of serial 10-fold dilutions of cells were spotted to YPD agar. The plates were incubated at the indicated temperatures and photographed after 2 d (30, 34 and 37°C), 3 d (25°C) or 4 d (20°C). (**C**) Primer extension analyses with ^{32}P-labeled primers complementary to U1 snRNA (nt 161–182) and U2 snRNA (nt 140–160) was performed using as template total cellular RNA isolated from the indicated *U1*Δ p(*CEN LEU2 U1*) strains. The reaction products were analyzed by denaturing PAGE and visualized by autoradiography. The sizes (nt) of ^{32}P-labeled marker DNAs that were analyzed in parallel are indicated at left.

Having shown that U1 snRNA tolerates installation of new RNA sequences upstream of the ^{3}ACUUAC^{8} sequence, we constructed a *tgs1*Δ *U1*Δ p(*CEN URA3 U1*) strain to test how separating the U1 cap from the 5′SS interaction element would affect *tgs1*Δ. To our surprise, rather than alleviating the *tgs1*Δ *cs* phenotype, the U1 5′ extensions exacerbated the impact of losing the TMG cap. A gradient of increasing synthetic sickness with *tgs1*Δ was seen for the *U1 +5*, *+25*, *+10* and *+20* alleles (Figure 2). The *+15* and *+30 U1* alleles were lethal in the *tgs1*Δ background.

Synthetic genetic interactions of the U1 5′ extensions

A possible explanation for the synthetic lethality/sickness of *tgs1*Δ with the 5′-extended U1s is that the effect of ectopic binding of CBC to the U1 m^{7}G cap in the *tgs1*Δ strain is more severe when the cap is distanced from the body of U1 by an otherwise benign 5′ RNA leader sequence (e.g. because the distance allows even freer access of CBC to the U1 cap at all growth temperatures). If this is the case, then we thought that the *cbc2-Y24A* mutation in the cap-binding pocket of nuclear CBC, which has no effect *per se* on yeast cell growth (Figure 2; *cbc2-Y24A U1-WT*) and which suppresses the *tgs1*Δ *cs* phenotype (Figure 2; *tgs1*Δ *cbc2-Y24A U1-WT*), might ameliorate the synergy between *tgs1*Δ and the 5′ U1 extensions. A necessary step *en route* to that issue was to query the effects of the U1 5′ extensions in a *cbc2-Y24A* background. This experiment revealed a gradient of synthetic sick and synthetic lethal interactions between *cbc2-Y24A* and the U1 mutant series, whereby the +5, +10, +20 and +25 extensions caused *cs* growth defects of increasing severity (reflected in the upward shift in the restrictive temperature) and the +15 and +30 extensions were lethal at all temperatures in the *cbc2-Y24A* background (Figure 2; *cbc2-Y24A*). Tyr24 in Cbc2 is the equivalent of Tyr20 in mammalian Cbc2 that forms a π–cation stack with the m^{7}G nucleobase to confer high-affinity cap binding. The synergistic effects of *cbc2-Y24A* with the altered U1 snRNAs seen here resonate with the recently reported synthetic lethality or sickness of *cbc2-Y24A* with null mutations of proteins involved in early steps of spliceosome assembly (Nam8, Mud1, Swt21, Mud2, Ist3 and Brr1) and with otherwise benign mutations of Msl5, the essential BP-binding protein (32). These combinatorial effects highlight how the contributions to spliceosome assembly of CBC engaged at the 5′ pre-mRNA cap are genetically buffered by other components of the splicing machinery. The present results identify the U1 snRNA 5′ end as a novel component of this genetic network. In light of the aforementioned findings, it was not surprising that the growth phenotypes of the 5′-extended *U1* alleles in the *tgs1Δ cbc-Y24A* background were virtually identical to those in the *tgs1*Δ background (Figure 2).

To delineate additional genetic interactions of the *U1* 5′ extensions, we constructed a series of yeast strains in which genes encoding inessential splicing factors were deleted in the *U1*Δ p(*CEN URA3 U1*) background, thereby allowing tests of synergy by plasmid shuffle. Although the ablation of U1 snRNP subunit Nam8 has no effect on yeast vegetative growth by itself, *nam8*Δ was lethal in combination with the *U1 +30* allele and caused a strong *cs* growth defect in combination with the five other *U1* 5′ extension alleles, manifest as no growth at 25°C, minimal growth at 30°C and varying degrees of slow growth at 34°C (Figure 2). The *U1* 5′ extensions had less of an impact in the absence of U1 snRNP subunit Mud1, whereby all alleles except *+30* were viable at 25°C in the *mud1*Δ background (Supplementary Figure S1). The *U1* 5′ extensions *+15*, *+20* and *+25* displayed *cs* synthetic sickness with a null mutation of the early splicing factor Swt21 that interacts genetically with CBC, Tgs1, Yhc1 and Prp28 (27,34); here, too the *U1 +30* allele had the most impact, with feeble growth at 25 and 20°C in the *swt21*Δ background (Supplementary

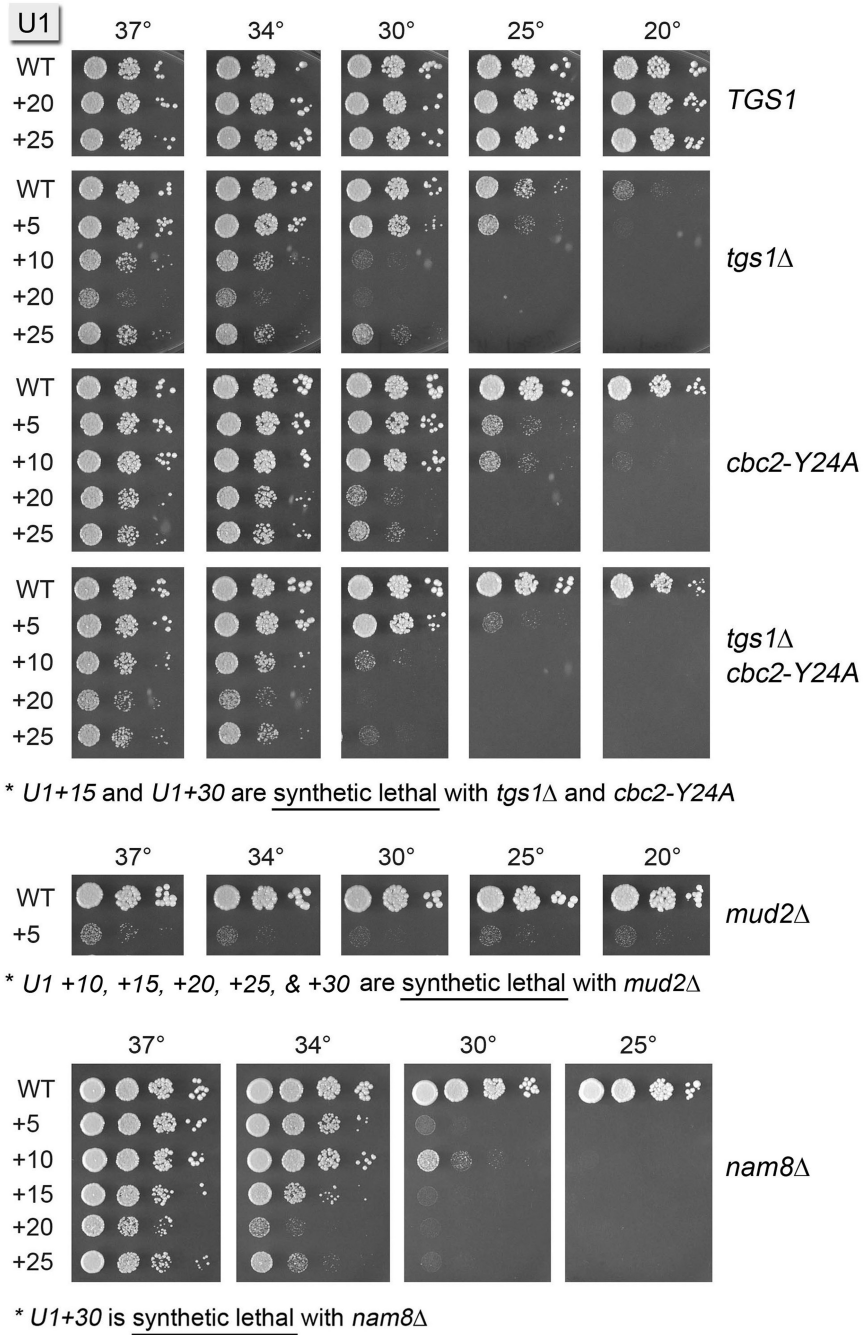

Figure 2. Synthetic genetic interactions of the U1 5′ extensions. Plasmid shuffle assays were used to test whether 5′ extended U1 snRNAs are functional in various genetic backgrounds. Synthetic lethality was indicated by failure to form macroscopic colonies on FOA agar after 10 d at 20, 30 and 37°C. Cultures of viable FOA-resistant cells were grown in YPD broth at 37°C and the growth phenotypes were assessed by spotting serial 10-fold dilutions as described in Figure 1B. The U1 alleles are specified on the left and the genetic background for the test of mutational synergy is indicated on the right.

Figure S1). The *U1 +20*, *+25*, and *+30* alleles grew poorly at 25 and 20°C in the absence of Brr1, a splicing factor implicated in snRNP biogenesis (35) (Supplementary Figure S1).

The strongest mutational synergies of the *U1* 5′ extensions were seen when the Mud2 subunit of the yeast heterodimeric BP-binding protein was ablated. Although *mud2*Δ cells grew normally with a *WT* U1 snRNA, the *U1 +5* allele was barely viable in the *mud2*Δ background, and the *+10*, *+15*, *+20*, *+25* and *+30* alleles were lethal (Figure 2). By contrast, the *U1* 5′ extensions displayed little or no synergy with a null mutation in Swm2 (Supplementary Figure S1), so named because *swm2*Δ is synthetic with *mud2*Δ (29).

Effects of insertions and deletions immediately downstream of the ^{3}ACUUAC^{8} sequence

The 5′ AUACUUACCU^{10} single-stranded segment of U1 snRNA precedes the folded U1 RNA tertiary structure that initiates at nucleotide U^{11} (i.e. a four-helix junction depicted in Figure 4A). The ^{8}CCU^{10} segment connecting the 5′SS complementary motif to helix 1 interacts with the U1-C subunit in the U1 snRNP (4,8). Here, we queried the importance of the spacing between the 5′SS complementary motif and helix 1 by introducing insertions of 1–30 nt between C^{8} and C^{9} (Figure 3). The insertion alleles were tested for bioactivity by plasmid shuffle in the *U1*Δ strain. The *[+1]* and *[+3]* insert strains were viable at 18–37°C, albeit slower growing than *WT U1* cells at low temperatures (Figure 3). By contrast, insertions of ≥5 nt between C^{8} and C^{9} were uniformly lethal (Figure 3). We performed primer extension analysis on RNA isolated from yeast cells with a wild-type chromosomal *U1* gene that had been transformed with *CEN* plasmids bearing the series of *U1* insertion alleles (Supplementary Figure S2). Denaturing PAGE analysis of the 5′ ^{32}P-labeled primer extension products revealed that the 5′ ends of the plasmid-encoded *[+1]*, *[+3]*, *[+5]*, *[+10]*, *[+20]* and *[+30]* U1 snRNAs were shifted incrementally upstream compared with the endogenous wild-type U1 snRNA. The levels of radiolabeled cDNAs derived from the U1 snRNA insertion mutants were at least as high as the cDNA corresponding to endogenous wild-type U1 snRNA (Supplementary Figure S2), signifying that (i) the steady-state levels of the U1 snRNA were not affected by the inserted sequences and (ii) the lethality of the *[+5]*, *[+10]*, *[+20]* and *[+30] U1* alleles was not attributable to a failure the produce the mutant snRNAs. We surmise that there are tight constraints on the length (and/or sequence) of the linker segment that interacts with U1-C. This theme was underscored as we systematically tested the viable *[+1]* and *[+3]* insert alleles for mutational synergies, which revealed that the *[+1]* and *[+3]* insertions were lethal in combination with *tgs1*Δ, *cbc2-Y24A*, *nam8*Δ, *mud1*Δ, *swt21*Δ and *mud2*Δ. Thus, even a single extra nucleotide sufficed to render U1 snRNA function dependent on otherwise inessential components of the U1 snRNP or the early spliceosome.

We also tested the effects of shortening the linker segment, by deleting nucleotides C^{9} and U^{10}, singly and in combination. The predicted 5′ structures of the deleted U1 RNAs are shown in Figure 4C. When tested by plasmid shuffle, the *U1* ΔC^{9} and $\Delta C^{9}U^{10}$ mutations were lethal. [Primer extension analysis showed that the mutant $\Delta C^{9}U^{10}$ U1 snRNA was synthesized from the plasmid-borne $\Delta C^{9}U^{10}$ gene *in vivo* and achieved steady-state levels at least as high as the chromosome-encoded wild-type U1 (Supplementary Figure S2).] By contrast, yeast *U1-*ΔU^{10} cells were viable and grew as well as *WT* cells at 37 and 34°C, but were slow growing at 25 and 20°C (Figure 4B). The *U1-*ΔU^{10} allele was synthetic lethal with *tgs1*Δ, *cbc2-Y24A*, *nam8*Δ, *mud1*Δ, *swt21*Δ and *mud2*Δ.

Effects of extending the base-pairing potential of helix 1

Helix 1 is conserved with respect to its presence and position in yeast and human U1 snRNAs but is not conserved at the level of primary structure. Whereas the 5′ strand of helix 1 in yeast U1 is ^{11}UAAGAU^{16} (Figure 4A), the corresponding segment of human helix 1 is ^{12}GCAGG^{16} (8). To probe the effects of increasing the length of yeast helix 1, we changed the ^{9}CU^{10} dinucleotide to ^{9}UA^{10}, thereby extending the base-pairing potential to the sequence at the 3′ end of U1 RNA such that helix 1 might span 8 bp instead of 6 bp (Figure 4A). This *U1* allele, named *H1L* ('helix 1 long'), supported normal yeast growth at all temperatures tested (Figure 4B). Though benign *per se*, the *H1L* mutant displayed a broad range of synthetic genetic interactions with other splicing factors. At the most severe end of the spectrum,

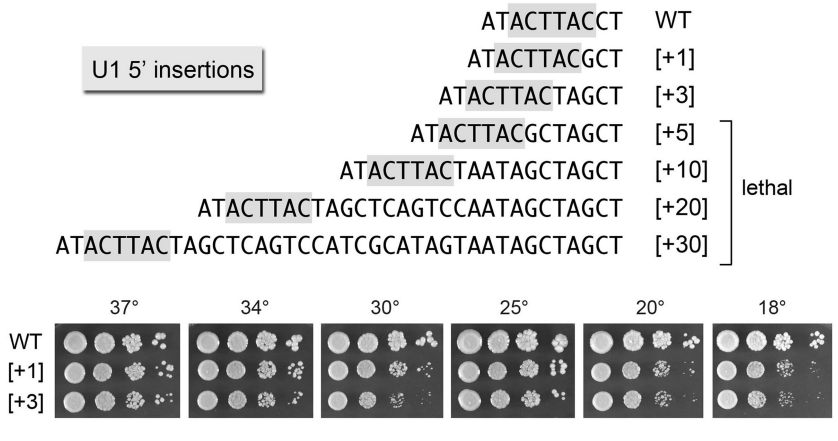

Figure 3. Effects of insertions immediately downstream of the ^{3}ACUUAC^{8} sequence. The DNA sequences are shown for the 5′ ends of WT U1 and the mutant variants *[+1]*, *[+3]*, etc., named according to the number of nucleotides inserted between positions C^{8} and C^{9}. The ^{3}ACTTAC^{8} segment that pairs with the intron 5′SS is highlighted in gray. The *[+5]*, *[+10]*, *[+20]* and *[+30]* mutants failed to complement *U1*Δ in a plasmid shuffle assay and were deemed lethal. The viable *U1-[+1]* and *U1-[+3]* strains were spot-tested for growth at the indicated temperatures in parallel with *WT* cells as per Figure 1B, except that the plates were incubated for 5 d at 25, 20 and 18°C. The synthetic lethal interactions of the *U1-[+1]* and *U1-[+3]* mutants are indicated at the bottom of the figure.

U1-H1L was synthetic lethal with *mud2*Δ. *H1L* was barely viable at 20–34°C in the *mud1*Δ background and did not grow at 37°C (Figure 4B). *H1L* synergized with *tgs1*Δ and *cbc2-Y24A*, resulting in feeble growth at 37 and 34°C and severe *cs* defects at the lower temperatures (Figure 4B). *H1L* caused slow growth at all temperatures in the *nam8*Δ and *swt21*Δ backgrounds (Figure 4B). These results show that increasing the size or stability of helix 1 enforces reliance on otherwise dispensable spliceosome components and assembly factors, especially Mud2.

Novel mutational effects in the ^{3}ACUUAC^{8} sequence

The base-pairing interaction between the 5′ end of yeast U1 snRNA and the consensus 5′SS of yeast pre-mRNAs is shown in Figure 5. Early studies of the effects of nucleobase changes within this segment of yeast U1 RNA identified the following lethal pyrimidine-to-purine mutations: *C4A*, *C4G*, *C8A* and *C8G* (36,37). Pyrimidine-to-pyrimidine mutants *C4U* and *C8U* were viable but slow growing at 30°C (36). The *U5A* allele, which eliminates a U:U mismatch in the U1•5′SS duplex (Figure 5), was also viable but slow growing at 30°C (36). Here, we examined the effects of these known viable mutations, and of several novel nucleobase changes in the ^{3}ACUUAC^{8} sequence, on the activity and genetic interactions of the U1 snRNA. The *C8U* mutant barely grew at 37 and 34°C and failed to grow at 25, 20 or 18°C (Figure 5A). The *C4U* strain grew best at 34°C and failed to grow at 25, 20 or 18°C (Figure 5A). We found that *C4U* was lethal at 34°C in combination with *tgs1*Δ, *cbc2-Y24A*, *nam8*Δ, *mud1*Δ, *swt21*Δ and *mud2*Δ. A new allele, *U1-A7G*, was viable but slow growing at 25, 30 and 34°C, but did not thrive at higher or lower temperatures (Figure 5A). *A7G* was inviable in combination with *tgs1*Δ, *cbc2-Y24A*, *nam8*Δ, *mud1*Δ, *swt21*Δ and *mud2*Δ.

New and instructive findings emerged from our analysis of mutations *U5A*, *U5G* and *U5C*. In agreement with Siliciano and Guthrie (36), we found that *U5A* cells were viable but modestly slow growing at all temperatures tested (Figure 5A). The *U5G* mutant was also viable and had virtually the same growth effects as *U5A* at higher temperatures but was slightly more affected at cold temperatures (Figure 5A). The *U5A* and *U5G* phenotypes could be caused by installation of a purine *per se* or to the establishment of an extra A:U or G:U base pair with the 5′SS in lieu of the native U:U mispair. Thus, it is remarkable that the *U5C* mutant grew as well as the *WT U1* strain at all temperatures (Figure 5A), signifying that a Py^{5}:U mispair in the U1•5′SS RNA hybrid suffices for seemingly normal U1 snRNA activity. A corollary of this result is that the characteristic pseudouridine

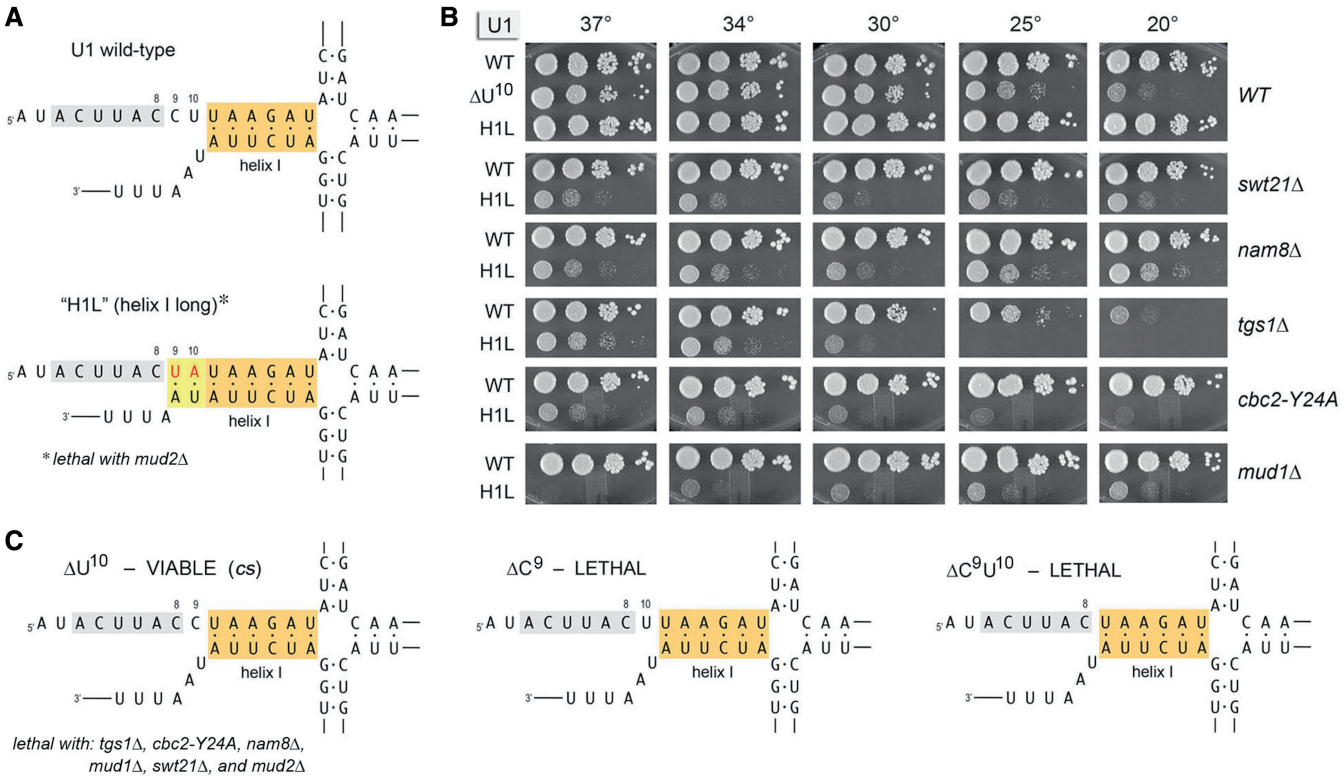

Figure 4. Effects of deletions immediately downstream of ^{3}ACUUAC^{8} and of extending the base-pairing potential of helix 1. (**A**) The primary and predicted secondary structures at the 5′ end of wild-type U1 RNA and the H1L mutant are shown. The ^{3}ACUUAC^{8} segment that pairs with the intron 5′SS is highlighted in gray. Helix 1 is shaded orange. The mutation of ^{9}CU^{10} to ^{9}UA^{10} (colored red) extends helix 1 by two base pairs, which are shaded yellow. (**B**) Yeast strains bearing *U1 WT*, *H1L* or *ΔU^{10}* alleles in the indicated genetic backgrounds were spot-tested for growth at the temperatures specified. (**C**) The primary and predicted secondary structures of the ΔU^{10}, ΔC^{9} and ΔC^{9}U^{10} deletion mutants of U1 snRNA are shown. The *ΔC^{9}* and *ΔC^{9}U^{10}* alleles failed to complement *U1*Δ and were deemed lethal. Genetic interactions of *H1L* and *ΔU^{10}* are indicated below the respective structures in (A) and (C).

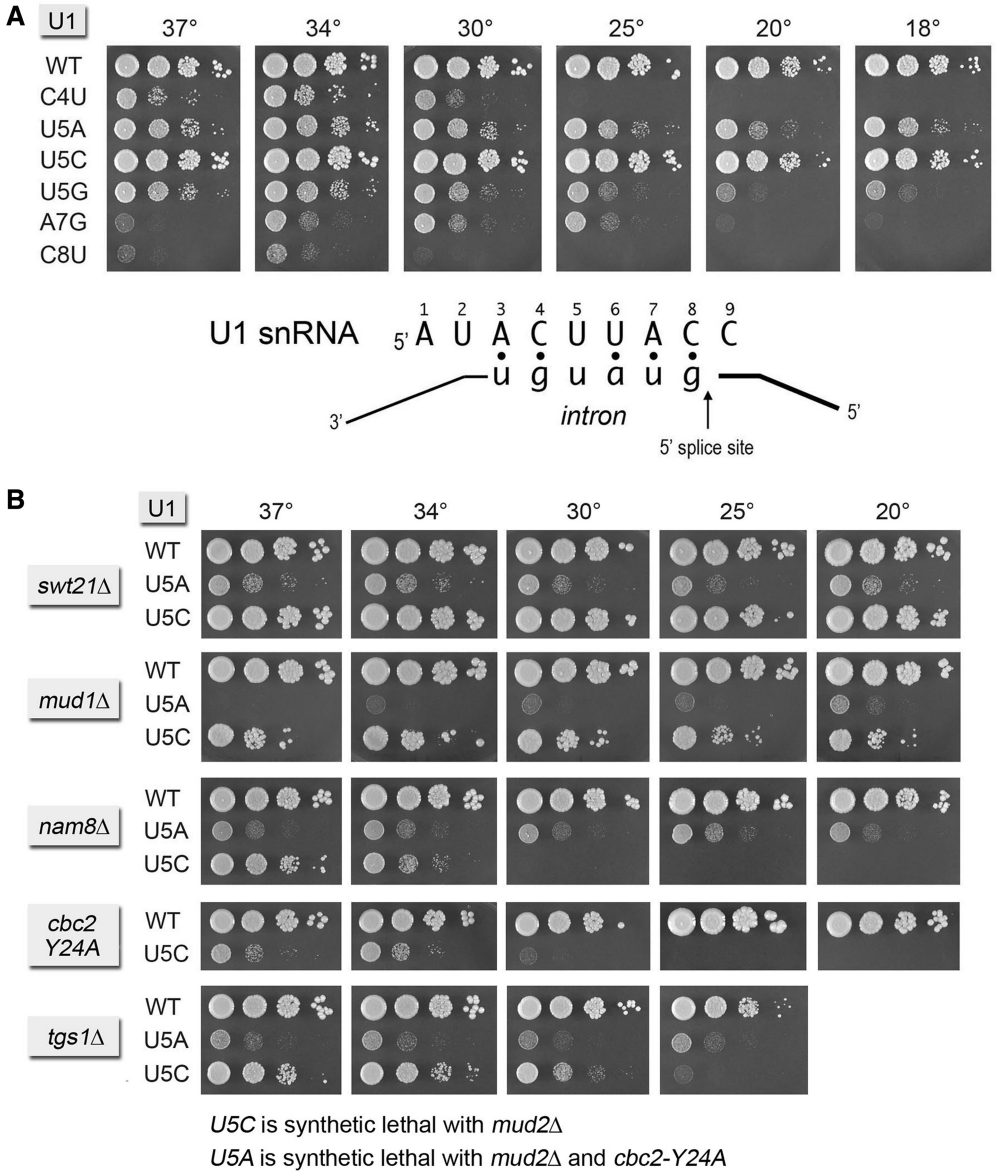

Figure 5. Effects of mutations in the ^{3}ACUUAC^{8} sequence. (**A**) The base-pairing interaction between the U1 snRNA ^{3}ACUUAC^{8} sequence and the consensus pre-mRNA 5′SS is shown. *U1*Δ p(*CEN LEU2 U1*) cells bearing the indicated *U1* alleles were spot-tested for growth at the indicated temperatures. (**B**) Yeast strains bearing *U1 WT*, *U5A* or *U5C* alleles in the indicated genetic backgrounds were spot-tested for growth at the temperatures specified. Synthetic lethal interactions of *U5A* and *U5C* are indicated at bottom.

modification of the U^{5} nucleobase in U1 snRNA (38) (which will not occur in the *U5C* mutant) is not critical for U1 snRNA function in an otherwise wild-type background.

We surveyed whether and how the function of the U1 snRNA *U5C* variant was affected by deleting optional splicing factors and U1 snRNP subunits. The U1 *U5C* mutation was unaffected by *swt21*Δ and displayed a mild synthetic growth defect with *mud1*Δ at all temperatures tested (Figure 5B). *U5C* exacerbated the *cs* phenotype of *tgs1*Δ, pushing the restrictive temperature upwards (Figure 5B). Strong genetic interactions of *U5C* were seen with *nam8*Δ and *cbc2-Y24A*, whereby the *U5C nam8*Δ and *U5C cbc2-Y24A* strains grew slowly at 37 and 34°C and failed to grow at 30, 25 and 20°C (Figure 5B). These results fortify the case for a role of Nam8 and cap binding by CBC in U1 snRNP assembly at a non-consensus 5′SS (30,32,39). The *U5C* allele was unconditionally synthetic lethal in the *mud2*Δ background (Figure 5B).

The same synergy tests were performed for the *U5A* snRNA mutant. The slow growth phenotype of *U5A* was evident at all temperatures in the *swt21*Δ and *tgs1*Δ backgrounds (Figure 5B). The same was true of *U5A nam8*Δ, thereby highlighting a distinctive genetic interaction of *nam8*Δ with *U5A* versus *U5C* in which the loss of Nam8 exerted a stronger growth effect on *U5C* (Figure 5B). *U5A* was synthetically lethal with *mud2*Δ and *cbc2-Y24A*.

New genetic interactions of Msl5 with subunits of the U1 snRNP, Mud2 and Cbc2

Saccharomyces cerevisiae Msl5 (BP-binding protein) orchestrates spliceosome assembly by binding the intron BP sequence 5′-UACUAAC and establishing cross-intron-bridging interactions with other components of the splicing machinery (20,22,31,40–42). Msl5 (a 476-aa polypeptide) is essential for yeast vegetative growth. The central BP RNA-binding domain of Msl5—composed of KH and QUA2 modules (43)—is flanked by N- and C-terminal domains that have imputed functions in protein–protein interactions. By gauging the ability of Msl5 mutants to complement *msl5*Δ, we recently reported that the Msl5 N-terminal Mud2-binding domain (aa 35–68) and a downstream $PPxY^{100}$ motif proposed to interact with WW-domain proteins (44) are inessential, as are a C-terminal proline-rich domain (aa 382–476) and two zinc-binding CxxCxxxxHxxxxC motifs (aa 273–286 and 299–312) (31). A subset of conserved BP RNA-binding amino acids in the central KH-QUA2 domain (aa 146–269) are essential pairwise (Ile189-Arg190; Leu256-Leu259) or in trios (Leu169-Arg172-Leu176), whereas other RNA-binding residues are dispensable (31). We have used our collection of viable Msl5 mutants to illuminate synthetic genetic interactions between Msl5 and Mud2, Nam8, Tgs1 and Cbc2 (31,32). The results suggested a network of important but functionally buffered protein–protein and protein–RNA interactions between the Msl5•Mud2 complex at the BP, U1 snRNP at the 5′SS and CBC at the pre-mRNA cap.

Here, we queried our collection of Msl5 mutants that have no growth defect *per se* for synthetic interactions with other components of the U1 snRNP not evaluated previously. We focused first on the Mud1 subunit. We found that *mud1*Δ was synthetically lethal with (i) an N-terminal truncation that eliminated part of the Mud2-binding site (aa 35–68); (ii) a triple-alanine mutation *P97A-P98A-Y100A* in the $PPxY^{100}$ motif; and (iii) a C-terminal truncation that eliminated aa 402–425 (Supplementary Table S1). Otherwise benign double-alanine mutations in the Msl5 KH-QUA2 domain were either lethal (*N163A-V165A*) or severely sick (*V195A-K196A*, *T265A-R267A* and *K252A-R253A*) in the *mud1*Δ background (Supplementary Table S1). By contrast, there was no synthetic lethality/sickness of *mud1*Δ with the *C273A–C276A* and *C299A–C302A* alleles that respectively disrupt the proximal and distal zinc knuckle modules of Msl5 (Supplementary Table S1).

To better delineate the essential constituents of the BP RNA binding site of yeast Msl5, we tested the effects of single alanine substitutions within the three lethal alanine-cluster alleles identified previously (31). Tests of *msl5*Δ complementation showed that: (i) *R172A*, *R190A* and *L259A* were unconditionally lethal; (ii) *L256A* displayed a tight *cs* growth phenotype; and (iii) *L169A*, *L176A* and *I189A* grew normally on YPD agar at all temperatures (Table 1). The NMR structure of human SF1 (the ortholog of Msl5) bound to an RNA (5′-AUACUAAC AA) containing the consensus yeast BP sequence (43) revealed an extensive network of atomic contacts between conserved amino acid side chains (many of them hydrophobic) and the RNA nucleobases and sugars, whereas the RNA phosphates are surface exposed and make relatively few protein contacts (Supplementary Figure S3). Given that six of the seven side chains mutated singly to alanine in Table 1 are identical in SF1 and Msl5 (Supplementary Figure S3), that the seventh Msl5 residue Leu169 is conserved as Ile in SF1, and that the RNA–protein contacts observed for these side chains in the SF1 structure are to a canonical yeast BP RNA recognition element, it is our presumption that the same RNA contacts are likely to be made by the equivalent Msl5 side chains. These contacts are listed in Table 1. (A complete list of the imputed BP RNA contacts made by all of the Msl5 residues that have been subjected to alanine scanning is provided in Supplementary Figure S4.) The striking finding is that only 4 of the 13 conserved side chains, and their imputed contacts to the BP (Supplementary Table S1), are essential for *msl5*Δ complementation.

We tested the three newly identified fully viable *MSL5* alleles for mutational synergies with mutations in other genes affecting early splicing events. *L176A* supported wild-type growth when combined with *mud1*Δ, *nam8*Δ, *mud2*Δ, *tgs1*Δ or *cbc2-Y24A* (Table 2). Thus, the inferred contacts of Leu176 with the BP adenosine (to the adenine N3 atom and the ribose O2′) are dispensable for yeast growth in all genetic backgrounds tested. By contrast, *L169A* and *I189A* were lethal in combination with *mud1*Δ, *nam8*Δ, *mud2*Δ, *tgs1*Δ or *cbc2-Y24A* (Table 2). Leu169 is imputed to intercalate between and make van der Waals contacts to the BP adenine and the upstream flanking adenine. Ile189 contacts the N1 and N6 atoms of the BP adenine. The emerging theme here is that the loss of U1 snRNP components, or weakening of CBC interactions with the mRNA cap, is buffered by cross-intron Msl5 contacts at the BP that, when weakened by mutations characterized presently, results in a failure of vegetative growth, presumably via insufficient splicing of one or more essential pre-mRNAs.

New genetic interactions of Msl5 with the 5′ end of U1 snRNA

Viable U1 snRNA mutants were tested for synthetic interactions with otherwise viable Msl5 mutations by constructing a *U1*Δ *msl5*Δ double knockout strain with a resident *CEN URA3 U1 MSL5* plasmid to sustain growth. This strain was co-transformed with various combinations of *CEN HIS3 MSL5* and *CEN LEU2 U1* plasmids, and individual His^+ Leu^+ transformants were tested for growth on FOA at 20, 30 and 37°C. Allelic pairs that failed to support growth on FOA at any temperature were deemed synthetic lethal (Table 3). FOA-resistant survivors were then grown in YPD liquid culture and tested for growth by spotting serial dilutions on YPD agar at 20, 25, 30, 34 and 37°C. The results are compiled in Table 3, wherein +++ signifies growth indistinguishable from wild-type *U1 MSL5* cells, ++ denotes smaller colony size and + indicates pinpoint colonies. Several of

Table 1. Effect of KH-QUA2 domain mutations on Msl5 function *in vivo*

MSL5	Contacts in BBP•RNA structure:	*msl5Δ* complementation			
Allele	$pU^1pA^2pC^3pU^4pA^5pA^6pC^7pA^8pA^9$	18°	25°	30°	37°
WT		+++	+++	+++	+++
L169A	**A^6** base; A^5 base	+++	+++	+++	+++
R172A	**A^6**pC^7 phosphate	–	–	–	–
L176A	**A^6** base N3, ribose O2′	+++	+++	+++	+++
I189A	**A^6** base N1 N6	+++	+++	+++	+++
R190A	A^9 base	–	–	–	–
L256A	A^2 ribose O2′; C^3 base N3, ribose O4′	–	–	+	++
L259A	U^4 base C2 O2, ribose O4′	–	–	–	–

Complementation of *msl5Δ* by the indicated *MSL5* alleles was assayed by plasmid shuffle (31). Individual Leu^+ transformants were streaked on agar medium containing FOA. Growth was scored after incubation for 7 d at 18, 25, 30 or 37°C. Lethal mutants were those that failed to form colonies at any temperature. Individual FOA-resistant colonies with viable *MSL5* alleles were grown to mid-log phase in YPD broth and adjusted to equivalent A_{600}. Aliquots (3 µl) of serial 10-fold dilutions were spotted on YPD agar plates, which were then incubated at 18, 25, 30 and 37°C. Growth was scored as follows: (+++) colony size was indistinguishable from strains bearing wild-type *MSL5*; (++) slightly reduced colony size; (+) only pinpoint macroscopic colonies were formed; (–) no growth.

Table 2. Synthetic interactions of Msl5 KH-QUA2 domain mutations

MSL5 allele	Complementation				
	mud1Δ	*mud2Δ*	*nam8Δ*	*cbc2-Y24A*	*tgs1Δ*
WT	+++	+++	+++	+++	+++
L169A	–	–	–	–	–
L176A	+++	+++	+++	+++	+++
I189A	–	–	–	–	–

Complementation of *msl5Δ* in the genetic backgrounds specified by otherwise functional *MSL5* alleles was assayed by plasmid shuffle. *L169A* and *I189A* transformants failed to form FOA-resistant colonies at any temperature tested in each of the five strain backgrounds. By contrast, *L176A* supported growth on FOA and, by spot testing, +++ growth on YPD agar at all temperatures in all five strains.

the allelic combinations elicited *ts* or *cs* growth failures; these are denoted as such in Table 3 next to the growth scores that applied to the permissive temperatures for these strains.

The *U1* 5′ extensions, the *U5C* mutation and the *H1L*, ΔU^{10} and *[+1]* changes distal to the 5′SS complementarity segment were uniformly synthetic lethal with *MSL5-(69–476)*, an N-terminal truncation that disrupts the interaction of the BP binding protein with Mud2/U2AF65 (42,45,46) (Table 3). Indeed, the synergies of *MSL5-(69-476)* with the U1 snRNA mutations phenocopied those of *mud2Δ* (Figures 2–5). By contrast, *MSL5-(55–476)*, which deletes only part of the Mud2-binding interface, permitted +++ growth of yeast bearing the 5′ extensions, *U5C* and *H1L* variants of U1 snRNA at low temperatures but did not support growth at 34–37°C (Table 3).

Lesions L169A and I189A in the RNA-binding site of Msl5 were synthetically lethal with most of the *U1* mutant alleles surveyed and, where the allelic pairs were viable, the cells were sick and cold-sensitive (Table 3). Other changes in the KH-QUA2 domain of Msl5 displayed less severe synthetic interactions with the U1 mutations. For example, *V195A K196A* and *K252R* elicited *cs* defects in combination with the *U1* 5′ extensions but displayed +++ or ++ growth at higher temperatures. The same *V195A K196A* and *K252R* alleles were lethal in combination with the ΔU^{10} and *[+1] U1* alleles (Table 3). At the other end of the spectrum, *MSL5-L176A* did not synergize with any of the 5′ extensions or *H1L*, but did display synthetic sickness with *[+1]* and ΔU^{10} (Table 3).

Dissecting the genetic interactions of the Msl5 $PPxY^{100}$ motif

The *msl5-(P97A-P98A-Y100A)* allele was synthetically lethal in combination with the 5′ extensions, *U5C*, ΔU^{10} and *[+1]* mutations in U1 snRNA (Table 3; $^{97}AAxA^{100}$). The *U1-H1L msl5-(P97A-P98A-Y100A)* strain was viable but slow growing and cold-sensitive (Table 3). The $PPxY^{100}$ motif was suggested to mediate a cross-intron-bridging interaction of Msl5 with the Prp40 subunit of the U1 snRNP (22). Prp40 is a 583-aa protein containing two tandem WW modules at the N-terminus (aa 1–70) and four FF domains dispersed downstream (44,47,48). The isolated tandem WW domain binds *in vitro* to a synthetic peptide PSP**PP**V**Y**DA corresponding to Msl5 residues 94–102 (44). A key question is whether the synthetic lethality of *P97A-P98A-Y100A* with mutations at the 5′ end of U1 snRNA is causally related to the loss of the imputed binding of the PPxY motif to the Prp40 WW domain. If this is the case, then deletion of the WW domain in Prp40 might phenocopy the mutational synergies of *msl5-(P97A-P98A-Y100A)*. We put this idea to the test by replacing the chromosomal *PRP40* locus with a truncated allele, *prp40-(77-583)* (henceforth named *prp40-ΔWW*), which cleanly subtracts the tandem WW modules. In agreement with the recent report by Görnemann *et al.* (49), we found that the *prp40-ΔWW* strain grew as well as the *PRP40* control strain on YPD agar at all temperatures (not shown). We proceeded to construct a *U1Δ prp40-ΔWW* p(*CEN URA3 U1*) strain suitable for plasmid shuffle of U1 snRNA variants. The instructive findings were that the *+5*, *+15*, *+20*, *+30* and *U5C* alleles of U1 that were synthetic lethal with *msl5-(P97A-P98A-Y100A)* were all viable in combination with *prp40-ΔWW* (Supplementary

Table 3. Synergies of U1 snRNA mutations with Msl5 mutations

U1 snRNA	*MSL5*							
	55–476	69–476	^{97}AAxA^{100}	L169A	L176A	I189A	V195 K196A	K252R
WT	+++	++	+++	+++	+++	+++	+++	+++
+5	+++	lethal	lethal	++ /cs[a]	+++	+	+++ /cs[b]	+++ /cs[c]
+15	+++ /ts[d]	lethal	lethal	lethal	+++	lethal	+++ /cs[e]	+++ /cs[c]
+20	+++ /ts[d]	lethal	lethal	+ /cs[f]	+++	lethal	+++ /cs[e]	++ /cs[a]
+30	+++ /ts[d]	lethal	lethal	lethal	+++	lethal	+++ /cs[e]	++ /cs[a]
U5C	+++ /ts[d]	lethal	lethal	lethal	+++	lethal	++ /cs[a]	++ /cs[a]
H1L	+++ /ts[d]	lethal	++ /cs[g]	lethal	+++	lethal	++ /cs[g]	+
ΔU^{10}	lethal	lethal	lethal	lethal	+	lethal	lethal	lethal
[+1]	+ /ts[h]	lethal	lethal	lethal	++	lethal	lethal	lethal

Complementation of *msl5Δ* in the *U1* genetic backgrounds specified was assayed by plasmid shuffle. Allelic combinations that failed to form colonies at any temperature are denoted as lethal. Viable strains were tested for growth on YPD agar and scored as described in Table 1. *ts* or *cs* phenotypes were as follows:
[a]++ at 34–37°C.
[b]+++ at 25–37°C.
[c]+++ at 34–37°C.
[d]+++ at 18–30°C.
[e]+++ at 30–37°C.
[f]+ at 34–37°C.
[g]++at 30–37°C.
[h]+ at 18–25°C.

Figure S5). The *prp40-ΔWW U1-U5C* strain grew well at all temperatures. *prp40-ΔWW* strains with *U1* 5′ extensions grew well at 37, 34 and 30°C but were slow growing at 20°C. The *prp40-ΔWW U1-H1L* strain grew slowly at all temperatures. These results are not compatible with a model whereby the severe synergies of the U1 snRNA 5′ mutations with *msl5-(P97A-P98A-Y100A)* are mediated exclusively (or predominantly) via the Prp40 WW domain. We surmise that the PPxY^{100} motif of Msl5 plays an important, albeit genetically buffered, role in pre-mRNA splicing that has naught to do with the Prp40 WW domain.

To better understand how the PPxY motif functions, we tested the effects of single mutations P97A, P98A and Y100A on Msl5 activity in several genetic backgrounds for which the *msl5-(P97A-P98A-Y100A)* triple-mutant was lethal (e.g. *mud1*Δ, *nam8*Δ, *cbc2-Y24A* and *tgs1*Δ) or sick (*mud2*Δ). Initial control experiments verified that the single mutations in PPxY had no impact on complementation of *msl5*Δ (not shown). Complementation tests for mutational synergies revealed that the *P97A* and *P98A* alleles had no genetic interactions with *mud1*Δ, *nam8*Δ, *cbc2-Y24A*, *tgs1*Δ or *mud2*Δ (Figure 6A). By contrast, the *Y100A* allele was synthetically lethal with *mud1*Δ and *nam8*Δ and synthetic sick with *mud2*Δ, effectively phenocopying the synthetic defects of the *^{97}AAxA^{100}* triple-mutant in these backgrounds (Figure 6A). *Y100A* was also synthetically sick with *cbc2-Y24A* and *tgs1*Δ (Figure 6A), as evinced by smaller colony size at 34 and 37°C and cold-sensitivity (Figure 6B). These results implicate the loss of Tyr100 as principally responsible for the synthetic interactions of the Msl5 ^{97}AAxA^{100} mutant with proteins involved in spliceosome assembly.

Tyr100 has been identified as a site of Msl5 phosphorylation *in vivo* (50). To probe whether the synthetic phenotypes of *msl5-Y100A* are related to the absence of tyrosine phosphorylation, we replaced Tyr100 with phenylalanine. The *Y100F* allele displayed no synthetic defects in combination with *mud1*Δ, *nam8*Δ, *cbc2-Y24A*, *tgs1*Δ or *mud2*Δ (Figure 6A). We conclude that the genetically buffered essential functions of Tyr100 are not related to its phosphorylation status.

We proceeded to test the effects of *P97A*, *P98A*, *Y100A* and *Y100F* in tandem with several *U1* alleles with which the *^{97}AAxA^{100}* triple-mutant was either synthetic lethal (i.e. *+5*, *+20*, *+30*, *U5C* and *[+1]*) or sick (*H1L*). *P97A* and *Y100F* sustained +++ growth in each *U1* mutant background at 20, 30, 34 and 37°C (not shown). *P98A* supported ++ growth at 20–37°C in the *+5*, *+20*, *+30*, *U5C* and *H1L* strains; the *msl5-P98A U1-[+1]* strain grew +++ at 30, 34 and 37°C and ++ at 20 and 25°C (not shown). By contrast, *msl5-Y100A* was sick in combination with *U1-[+1]* and *+30*. The *msl5-Y100A U1-[+1]* strain formed pinpoint colonies at 37 and 30°C and failed to grow at 25 or 20°C (Supplementary Figure S6). The *msl5-Y100A U1 +30* strain also grew slowly at high temperature and did not grow at low temperature (Supplementary Figure S6). *Y100A* displayed a *cs* growth defect in combination with the *+20* 5′ extension but had little or no synthetic phenotype with *U1-H1L* and *+5* (Supplementary Figure S6). Thus, the loss of Tyr100 sufficed to synergize with otherwise benign mutations of the U1 snRNA, albeit as a *forme fruste* of the impact of *^{97}AAxA^{100}* in these mutant *U1* backgrounds.

Bypass of the essentiality of Prp28 by U1 snRNA mutations

Yeast Prp28 is an essential pre-mRNA splicing factor and a member of the DEAD-box family of nucleic acid-dependent NTPases (51,52). Although Prp28 has been imputed to be an RNA helicase, the catalytic activities inherent to yeast Prp28 have not been characterized.

A

^{97}PPxY^{100}	Complementation				
	mud1Δ	*mud2Δ*	*nam8Δ*	*cbc2-Y24A*	*tgs1Δ*
P97A	+++	+++	+++	+++	+++
P98A	+++	+++	+++	+++	+++
Y100A	lethal	++ /*cs*	lethal	++ /*cs*	++ /*cs*
Y100F	+++	+++	+++	+++	+++
^{97}AAxA^{100}	lethal	++ /*cs*	lethal	lethal	lethal

B

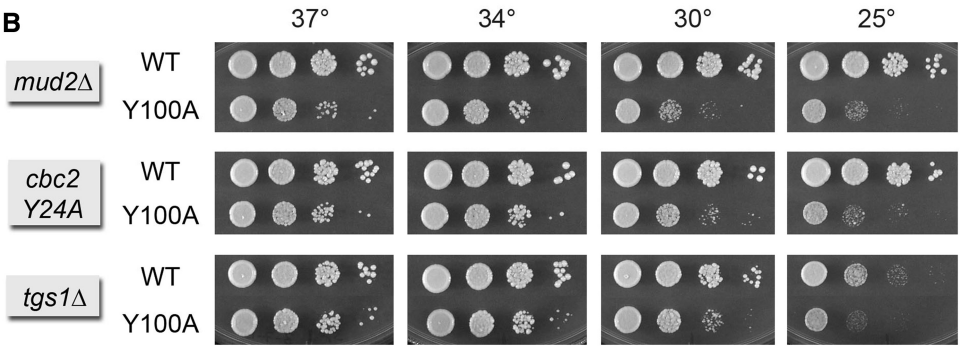

Figure 6. Genetic interactions of the Msl5 PPxY^{100} motif. (**A**) Complementation of *msl5Δ* by the indicated *MSL5* alleles was assayed by plasmid shuffle. Individual Leu^{+} transformants were streaked on agar medium containing FOA. Growth was scored after incubation for 7 d at 18, 25, 30 or 37°C. Lethal mutants were those that failed to form colonies at any temperature. Individual FOA-resistant colonies with viable *MSL5* alleles were grown to mid-log phase in YPD broth and adjusted to equivalent A_{600}. Serial 10-fold dilutions were spotted on YPD agar plates, which were then incubated at 25, 30, 34 and 37°C. Growth was scored as follows: (+++) colony size indistinguishable from strains bearing wild-type *MSL5* at all temperatures; (++) slightly reduced colony size; (*cs*) pinpoint colonies at 25°C. (**B**) Spot testing of the growth of *MSL5 WT* versus *Y100A* in the indicated strain backgrounds at the temperatures specified.

Nonetheless, Prp28 is implicated genetically in displacement of the U1 snRNP from the 5′SS during the transition from a pre-mRNA•U1•U2-containing spliceosome to a pre-mRNA•U2•U5•U6 spliceosome (15,16,34). Initial insights came from the observation that the deleterious effects of hyper-stabilizing the U1•5′SS base-paring interaction were genetically enhanced by a *cs* mutant of *prp28*, but not by conditional mutants of six other helicase-like splicing factors (16). In turn, the *prp28-cs* phenotype could be suppressed by an extra U1 snRNA gene with a *C4U* change that weakens its base-pairing to the consensus 5′SS (16). The case was fortified by the finding that the essentiality of Prp28 for vegetative growth could be bypassed by mutations in the essential U1 snRNP subunits Yhc1, Prp42 and Snu71, but not by deletions of the inessential subunits Nam8 and Mud1 (15,34). Deletion of the splicing factor Swt21 also rescued the lethality of *prp28*Δ (34). These results highlighted that the need for Prp28 during U1 snRNP ejection from the early spliceosome is alleviated by certain alterations that are presumed to weaken U1•5′SS contacts. This idea was consolidated by the demonstration that ectopic expression of mutant U1 snRNAs C4U, U5C or C8U (on top of a wild-type U1 snRNA) could also restore viability to *prp28*Δ (15).

Here, we surveyed our collection of viable U1 snRNA mutants for Prp28 bypass, by constructing a *U1*Δ *prp28*Δ double-knockout strain with a resident *CEN URA3 U1 PRP28* plasmid to sustain growth. This strain was transformed with *CEN LEU2 U1* plasmids, and the transformants were screened for growth on FOA at 18–37°C such that only *U1* variants that bypass the Prp28 requirement will give rise to FOA-resistant colonies. The important distinction between this and prior tests of *U1* bypass of Prp28 is that our assay mandates that the *U1* variants bypass *prp28*Δ when they are the only source of U1 snRNA in the cell. Four U1 snRNA mutants passed this test: *C4U*, *U5C*, *ΔU^{10}* and *[+3]*. The viable *U1*Δ *prp28*Δ cells bearing these bypass *U1* alleles were tested for growth on YPD agar at 20, 25, 30, 34 and 37°C (Figure 7).

The hierarchy of bypass strengths was noteworthy. The *ΔU^{10}* variant of U1 snRNA was the best of the Prp28 bypass suppressors, insofar as *ΔU^{10} prp28*Δ cells grew about as well as wild-type cells at 37, 34 and 30°C, as gauged by colony size (Figure 7). The progressive *cs* growth defect of the *ΔU^{10} prp28*Δ strain at 25 and 20°C (Figure 7) was exactly what was seen for the *ΔU^{10} PRP28* mutant strain (Figure 4, ΔU^{10} WT). Thus, *ΔU^{10}* appears to be fully independent of Prp28.

U5C was the next best of the Prp28 bypass suppressors. *U5C prp28*Δ cells grew at 37, 34 and 30°C, albeit slower than the wild-type strain, and were unable to grow at 20°C (Figure 7). Because the U5C snRNA supported apparently normal growth at all temperatures in a *PRP28* background (Figure 5A), we surmise that the bypass effect of *U5C* is cold-sensitive. This result suggests that higher temperatures help destabilize already weakened U1-U5C•5′SS pairing and thereby permits U1 snRNP ejection without

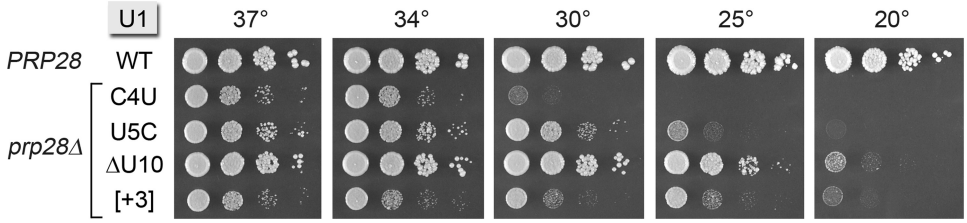

Figure 7. U1 mutations bypass the requirement for the essential *PRP28* gene. Yeast *prp28*Δ *U1*Δ cells harboring the indicated *U1* allele—*WT*, *C4U*, *U5C*, *ΔU*[10] or *[+3]*—on a *CEN LEU2* plasmid and either wild-type *PRP28* (*CEN HIS3*) or an empty *CEN HIS3* plasmid (*prp28*Δ) were grown in liquid cultures at 37°C to mid-log phase. The cultures were adjusted to A_{600} of 0.1, and aliquots of serial dilutions were spotted to YPD agar. Photographs of the plates after incubation for 2 d (30, 34, 37°C), 4d (25°C) or 5 d (20°C) are shown.

the assistance of Prp28. However, when the pairing is more stable at lower temperatures, Prp28 is still required.

Although *C4U* appeared to be less effective in Prp28 bypass when comparing growth of *C4U prp28*Δ to the wild-type strain (Figure 7), bear in mind that *C4U per se* elicits the same phenotype in a *PRP28* background (Figure 5). (Side-by-side comparisons of the *C4U PRP28* and *C4U prp28*Δ strains revealed no difference in growth; not shown.)

The *[+3]* insertion between the 5′SS complementarity motif and the first hairpin restored slow growth to *prp28*Δ cells at 37, 34, 30 and 25°C but did not bypass at 20°C (Figure 6). Because the *[+3]* insertion did not cause a strong *cs* phenotype in the *PRP28* background (Figure 3 and side-by-side growth comparisons not shown), we conclude that the *[+3]* bypass effect is cold-sensitive, *à la U5C*.

DISCUSSION

The present study reveals structure–function relationships at the 5′ end of the yeast U1 snRNA and their contributions to an expansive network of genetic interactions among proteins and RNA elements that drive spliceosome assembly. We show that the 5′ dinucleotide leader between the TMG cap and the conserved ^{3}ACUUAC^{8} motif can be enlarged by 30 nt without compromising cell growth. By contrast, there are tight functional constraints on the downstream dinucleotide spacer between ^{3}ACUUAC^{8} and helix 1 of the U1 snRNA fold, whereby insertions of ≥5 nt are lethal. We exploited our collection of biologically active U1 alleles with 5′ extensions, variations in the ^{3}ACUUAC^{8} sequence, short downstream insertions/mutations and a longer H1 helix to discover new intra-snRNP synergies with the inessential U1 components Nam8, Mud1 and the TMG cap. We also found new synergies with the non-snRNP splicing factor complexes Msl5•Mud2 and CBC that bind the intron BP and pre-mRNA 5′ cap, respectively. These results fortify the idea that spliceosome assembly can be facilitated by any of several genetically buffered microscopic pathways involving cross-intron-bridging interactions of the U1 snRNP•5′SS complex with the Mud2•Msl5•BP complex and cross-exon-bridging interactions of the CBC•m^{7}GpppRNA complex with the U1•5′SS complex. Although elimination or weakening of one set of interactions by deletions of inessential components or missense mutations in essential components can be tolerated at the level of vegetative growth, the effects of simultaneous subtraction of functionally overlapping microscopic pathways are seen as synthetic lethality or sickness.

The composition of the U1 snRNP is much more complex in budding yeast than in mammals, with respect to the size of the U1 RNA (568 versus 164 nt) and the number of U1-specific protein subunits (10 versus 3). The larger yeast U1 RNA may include binding sites for some of the yeast-specific U1 subunit proteins, which are Prp39, Prp40, Snu71, Snu56, Luc7, Prp42 and Nam8. Mammalian cells have putative homologs of Luc7 (hLuc7), Nam8 (TIA-1) and Prp40 (FBP11) (1,13,53), but they are not subunits of the U1 snRNP. By assimilating these seven yeast proteins as stoichiometric subunits, the yeast U1 snRNP can serve as a recipient of splicing regulation (via signals in the pre-mRNA or interactions with other splicing factors) that, in the case of mammalian splicing, are conveyed by an armada of *trans*-acting splicing factors that influence 5′SS usage and/or formation of the U1•5′SS complex (54,55), most of which have no equivalents in budding yeast.

The present study is informative regarding the cross-intron contacts between the U1•5′SS and Mud2•Msl5•BP complexes, via our analysis of the effects of mutations in the BP-binding protein Msl5. Because Msl5 is essential in budding yeast, and because mutational analyses of the yeast intron BP have focused almost exclusively on base-pairing interactions with the U2 snRNP (56–58), there is little known about the necessity and function of Msl5•BP interactions *in vivo*. Here, we extended our initial structure-guided mutagenesis of the RNA-binding site of Msl5 to consolidate the following points. First, that alanine mutations of only four of the Msl5 amino acids that contact the consensus BP are unconditionally or conditionally lethal: Arg172, Arg190, Leu256 and Leu259. By contrast, alanine mutations of nine other Msl5 amino acids that contact the consensus BP elicit no growth phenotypes. However, we found allele-specific synergies of otherwise benign RNA-binding site mutations with mutations in the U1 snRNA, U1 snRNP subunits Mud1 and Nam8, Tgs1, Mud2 and Cbc2. These results discriminate essential from optional BP RNA contacts and imply that the effects of hypomorphic Msl5 changes that weaken BP binding are buffered by interactions with the U1 snRNP that are mediated, at least in part, via the Mud2 subunit of the Msl5•Mud2 heterodimer.

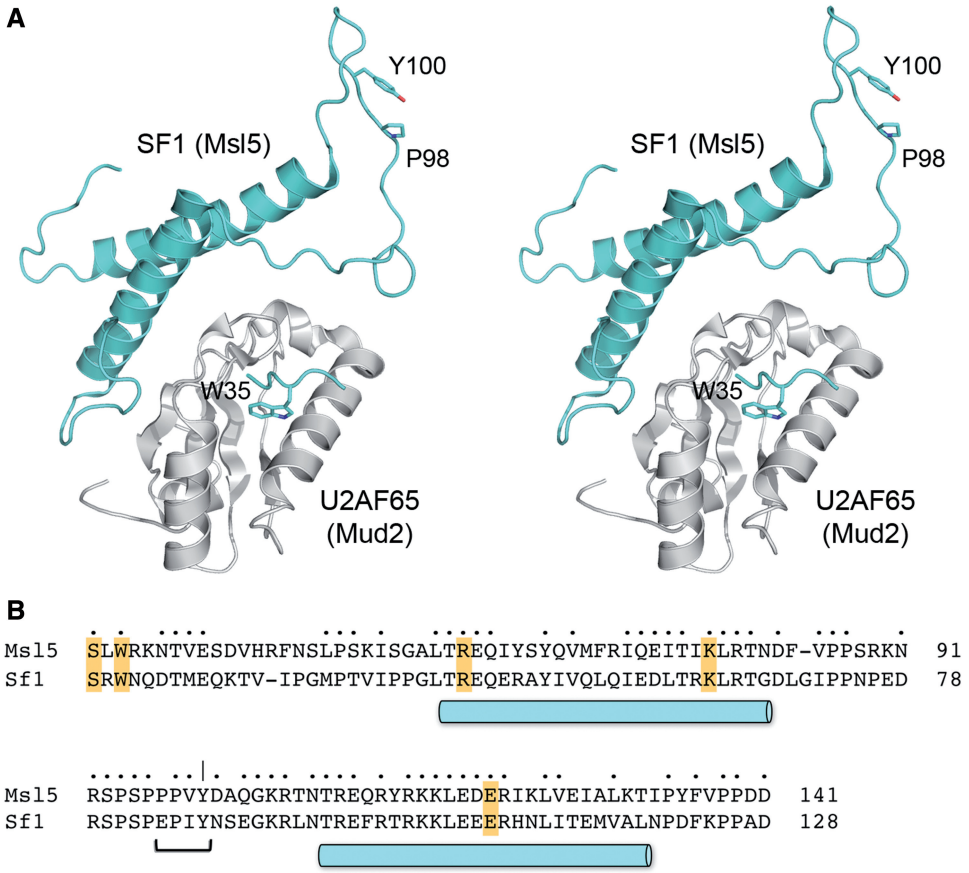

Figure 8. Disposition of PxY^{100} in the structure of SF1 bound to U2AF65. (**A**) Stereo view of the crystal structure (pdb 4FXW) of the complex between SF1-(20-128) (colored cyan) and the U2AF65 RRM3 domain (colored gray). Selected SF1 side chains are shown a stick models and are numbered according to their positions in yeast Msl5. (**B**) Alignment of the amino acid sequences of the N-terminal domains of Msl5 and SF1, corresponding to the SF1 structure shown in (A). Positions of side chain identity/similarity are indicated by •. The two α-helices comprising the coiled-coil of SF1 are indicated by cylinders below the alignment. The PPxY motif in the connecting loop is denoted by a bracket.

The N-terminal domains of Msl5 and human SF1 are responsible for interactions with the C-terminal RRM3 domains of Mud2 and U2AF65, respectively. Initial structural studies identified an SF1 peptide segment (^{13}PSKKRKRSRWNQD^{25}) that bound U2AF65, with the principal contact point being the insertion of a conserved SF1 tryptophan side chain (Trp22 in SF1; Trp35 in Msl5) into a hydrophobic pocket of U2AF65 (59) (see Figure 8). Although this SF1 segment is conserved in yeast Msl5, mutational studies showed that the Msl5 W35A change did not phenocopy the synthetic genetic interactions of *mud2*Δ (31). Moreover, compound mutations of the conserved Mud2 amino acids that, in U2AF65, comprise the SF1 peptide-binding site did not affect Mud2 function *in vivo* in genetic backgrounds where Mud2 is essential (31). These results suggested that the Mud2•Msl5 interface might be more complex than that seen in the U2AF65•SF1 peptide structure. The detailed anatomy of the SF1•USAF65 interface (and by extension the Mud2•Msl5 interface) has since been clarified by X-ray and NMR structures of a complex between SF1-(20-128) and the U2AF65 RRM3 (45,46). RRM3 interacts with a newly defined domain module of SF1, composed of two long α-helices that form an antiparallel coiled coil (Figure 8A). The SF1 α-helices include several side chains that contact U2AF65 directly. Because these side chains are conserved in yeast Msl5 (highlighted in Figure 8B), we presume they comprise a homologous interface with Mud2. The salient point we take from the new SF1–U2AF65 structure is that the equivalent of the Msl5 ^{97}PPxY^{100} motif (^{84}EPxY^{87} in SF1) is located within the loop that connects the two α-helices and is not a component of the interface with Mud2/U2AF65 (Figure 8A). Our studies here show that the aromatic Tyr100 residue of the Msl5 loop plays an important role *in vivo* that is revealed when the other splicing factors or the U1 snRNA are absent or mutated. The earlier suggestion from *in vitro* studies that the PPxY peptide of Msl5 mediates Msl5 binding to the WW domains of Prp40 is not consistent with our findings here that deletion of the WW domain in Prp40 did not phenocopy the mutational synergies of *msl5-(P97A-P98A-Y100A)* with U1 alleles (Supplementary Figure S4). Also, we noted that a *prp40-ΔWW mud1*Δ strain displayed wild-type growth at all temperatures (not shown), in contrast to the unconditional synthetic lethality of *msl5-(P97A-P98A-Y100A) mud1Δ* (Supplementary Table S1). The location of Tyr100 on an exposed surface of the loop distant from

the putative Mud2-Msl5 interface (Figure 8A) suggests that Tyr100 mediates the interaction of Msl5 with another component of the yeast splicing apparatus, either a domain of Mud2 or Msl5 not present in the SF1-U2AF65 structure, or a component of the U1 snRNP, or yet another splicing factor.

SUPPLEMENTARY DATA

Supplementary Data are available at NAR Online: Supplementary Table 1 and Supplementary Figures 1–6.

FUNDING

National Institutes of Health (NIH) [GM52470 to S.S.] and [GM50288 to B.S.]. S.S. is an American Cancer Society Research Professor. B.S. is a recipient of a Hearst Foundation Award. Funding for open access charge: NIH [GM52470].

Conflict of interest statement. None declared.

REFERENCES

1. Fabrizio,P., Dannenberg,J., Dube,P., Kastner,B., Stark,H., Urlaub,H. and Lührmann,R. (2009) The evolutionarily conserved core design of the catalytic activation step of the yeast spliceosome. *Mol. Cell*, **36**, 593–608.
2. Warlocki,Z., Odenwälder,P., Schitzova,J., Platzmann,F., Stark,H., Urlaub,H., Ficner,R., Fabrizio,P. and Lührmann,R. (2009) Reconstitution of both steps of *Saccharomyces cerevisiae* splicing with purified spliceosomal components. *Nat. Struct. Mol. Biol.*, **16**, 1237–1243.
3. Hoskins,A.A., Friedman,L.J., Gallagher,S.S., Crawford,D.J., Anderson,E.G., Wombacher,R., Ramirez,N., Cornish,V.W., Gelles,J. and Moore,M.J. (2011) Ordered and dynamic assembly of single spliceosomes. *Science*, **331**, 1289–1295.
4. Tang,J., Abovich,N., Fleming,M.J., Séraphin,B. and Rosbash,M. (1997) Identification and characterization of a yeast homolog of U1 snRNP-specific protein C. *EMBO J.*, **13**, 4082–4091.
5. Gottschalk,A., Tang,J., Puig,O., Salgado,J., Neubauer,G., Colot,H.V., Mann,M., Séraphin,B., Rosbash,M. and Lührmann,R. (1998) A comprehensive biochemical and genetic analysis of the yeast U1 snRNP reveals five novel proteins. *RNA*, **4**, 374–393.
6. Fortes,P., Bilbao-Cortés,D., Fornerod,M., Rigaut,G., Raymond,W., Séraphin,B. and Mattaj,I.W. (1999) Luc7p, a novel yeast U1 snRNP protein with a role in 5′ splice site recognition. *Genes Dev.*, **13**, 2425–2438.
7. Schwer,B., Erdjument-Bromage,H. and Shuman,S. (2011) Composition of yeast snRNPs and snoRNPs in the absence of trimethylguanosine caps reveals nuclear cap binding protein as a gained U1 component implicated in the cold-sensitivity of *tgs1*Δ cells. *Nucleic Acids Res.*, **39**, 6715–6728.
8. Pomeranz Krummel,D.A., Oubridge,C., Leung,A.K.W., Li,J. and Nagai,K. (2009) Crystal structure of human spliceosomal U1 snRNP at 5.5 Å resolution. *Nature*, **458**, 475–480.
9. Weber,G., Trowitzsch,S., Kastner,B., Lührmann,R. and Wahl,M.C. (2010) Functional organization of the Sm core in the crystal structure of human U1 snRNP. *EMBO J.*, **29**, 4172–4184.
10. Leung,A.K.W., Nagai,K. and Li,J. (2011) Structure of the spliceosomal U4 snRNP core domain and its implications for snRNP biogenesis. *Nature*, **473**, 536–539.
11. Van der Feltz,C., Anthony,K., Brilot,A. and Pomeranz Krummel,D.A. (2012) Architecture of the spliceosome. *Biochemistry*, **51**, 3321–3333.
12. Zhang,D. and Rosbash,M. (1999) Identification of eight proteins that cross-link to pre-mRNA in the yeast commitment complex. *Genes Dev.*, **13**, 581–592.
13. Puig,O., Bragado-Nilsson,E., Koski,T. and Séraphin,B. (2007) The U1 snRNP-associated factor Luc7p affects 5′ splice site selection in yeast and human. *Nucleic Acids Res.*, **35**, 5874–5885.
14. Lewis,J.D., Görlich,D. and Mattaj,I.W. (1996) A yeast cap binding protein complex (yCBC) acts at an early step in pre-mRNA splicing. *Nucleic Acids Res.*, **24**, 3332–3336.
15. Chen,J.Y., Stands,L., Staley,J.P., Jackups,R.R., Latus,L.J. and Chang,T.H. (2001) Specific alterations of U1-C protein or U1 small nuclear RNA can eliminate the requirement of Prp28p, an essential DEAD box splicing factor. *Mol. Cell*, **7**, 227–232.
16. Staley,J.P. and Guthrie,C. (1999) An RNA switch at the 5′ splice site requires ATP and the DEAD box protein Prp28p. *Mol. Cell*, **3**, 55–64.
17. Siliciano,P.G., Kivens,W.J. and Guthrie,C. (1991) More than half of yeast U1 snRNA is dispensable for growth. *Nucleic Acids Res.*, **19**, 6367–6372.
18. Liao,X., Kretzner,L., Séraphin,B. and Rosbash,M. (1990) Universally conserved and yeast-specfic U1 snRNA sequences are important but not essential for U1 snRNP function. *Genes Dev.*, **4**, 1766–1774.
19. Liao,X.C., Tang,J. and Rosbash,M. (1991) An enhancer screen identifies a gene that encodes the yeast U1 snRNP A protein: implications for snRNP protein function in pre-mRNA splicing. *Genes Dev.*, **7**, 419–428.
20. Abovich,N., Liao,X.C. and Rosbash,M. (1994) The yeast MUD2 protein: an interaction with PRP11 defines a bridge between commitment complexes and U2 snRNP addition. *Genes Dev.*, **8**, 843–854.
21. Colot,H.V., Stutz,F. and Rosbash,M. (1996) The yeast splicing factor Mud13p is a commitment complex component and corresponds to CBP20, the small subunit of the nuclear cap-binding complex. *Genes Dev.*, **10**, 1699–708.
22. Abovich,N. and Rosbash,M. (1997) Cross-intron bridging interactions in the yeast commitment complex are conserved in mammals. *Cell*, **89**, 403–412.
23. Tang,J., Abovich,N. and Rosbash,M. (1996) Identification and characterization of a yeast gene encoding the U2 small nuclear ribonucleoprotein particle B'' protein. *Mol. Cell. Biol.*, **16**, 2787–2795.
24. Fortes,P., Kufel,J., Fornerod,M., Polycarpou-Schwarz,M., Lafontaine,D., Tollervey,D. and Mattaj,I.W. (1999) Genetic and physical interaction involving the yeast nuclear cap-binding complex. *Mol. Cell. Biol.*, **19**, 6543–6553.
25. Tong,A.H., Evangelista,M., Parsons,A.B., Xu,H., Bader,G.D., Page,N., Robinson,M., Raghibizadeh,S., Hogue,C.W. and Bussey,H. (2001) Systematic genetic analysis with ordered arrays of yeast deletion mutants. *Science*, **294**, 2364–2368.
26. Wilmes,G.M., Bergkessel,M., Bandyopadhyay,S., Shales,M., Braberg,H., Cagney,G., Collins,S.R., Whitworth,G.B., Kress,T.L. and Weissman,J.S. (2008) A genetic interaction map of RNA-processing factors reveals links between Sem1/Dss1-containing complexes and mRNA export and splicing. *Mol. Cell*, **32**, 735–746.
27. Hausmann,S., Zheng,S., Costanzo,M., Brost,R.L., Garcin,D., Boone,C., Shuman,S. and Schwer,B. (2008) Genetic and biochemical analysis of yeast and human cap trimethylguanosine synthase: functional overlap of TMG caps, snRNP components, pre-mRNA splicing factors, and RNA decay pathways. *J. Biol. Chem.*, **283**, 31706–31718.
28. Costanzo,M., Baryshnikova,A., Bellay,J., Kim,Y., Spear,E.D., Sevier,C.S., Ding,H., Koh,J.L., Toufighi,K., Mostafavi,S. *et al.* (2010) The genetic landscape of a cell. *Science*, **327**, 425–431.
29. Chang,J., Schwer,B. and Shuman,S. (2010) Mutational analyses of trimethylguanosine synthase (Tgs1) and Mud2: proteins implicated in pre-mRNA splicing. *RNA*, **16**, 1018–1031.
30. Qiu,Z.R., Schwer,B. and Shuman,S. (2011) Determinants of Nam8-dependent splicing of meiotic pre-mRNAs. *Nucleic Acids Res.*, **39**, 3427–3445.
31. Chang,J., Schwer,B. and Shuman,S. (2012) Structure-function analysis and genetic interactions of the yeast branchpoint binding protein Msl5. *Nucleic Acids Res.*, **40**, 4539–4552.

32. Qiu,Z.R., Chico,L., Chang,J., Shuman,S. and Schwer,B. (2012) Genetic interactions of hypomorphic mutations in the m^7G cap binding pocket of yeast nuclear cap binding complex: an essential role for Cbc2 in meiosis via splicing of *MER3* pre-mRNA. *RNA*, **18**, 1996–2011.
33. Schwer,B., Mao,X. and Shuman,S. (1998) Accelerated mRNA decay in conditional mutants of yeast mRNA capping enzyme. *Nucleic Acids Res.*, **26**, 2050–2057.
34. Hage,R., Tung,L., Du,H., Stands,L., Rosbash,M. and Chang,T.H. (2009) A targeted bypass screen identifies Ynl187p, Prp42p, Snu71p, and Cbp80p for stable U1 snRNP/pre-mRNA interaction, *Mol. Cell. Biol.*, **29**, 3941–3952.
35. Noble,S.M. and Guthrie,C. (1996) Transcriptional pulse-chase analysis reveals a role for a novel snRNP-associated protein in the manufacture of spliceosomal snRNPs. *EMBO J.*, **15**, 4368–4379.
36. Siliciano,P.G. and Guthrie,C. (1988) 5′ splice site selection in yeast: genetic alterations in base-pairing with U1 reveal additional requirements. *Genes Dev.*, **2**, 1258–1267.
37. Séraphin,B., Kretzner,L. and Rosbash,M. (1988) A U1 snRNA:pre-mRNA base pairing interaction is required early in yeast spliceosome assembly but does not uniquely define the 5′ cleavage site. *EMBO J.*, **7**, 2533–2538.
38. Massenet,S., Motorin,Y., Lafontaine,D.L.J., Hurt,E.C., Grosjean,H. and Branlant,C. (1999) Pseudouridine mapping in the *Saccharomyces cerevisiae* spliceosomal U small RNAs (snRNAs) reveals that pseudouridine synthase Pus1p exhibits a dual substrate specificity for U2 snRNA and tRNA. *Mol. Cell. Biol.*, **19**, 2142–2154.
39. Spingola,M. and Ares,M. (2000) A yeast intronic splicing enhancer and Nam8p are required for Mer1p-activated splicing. *Mol. Cell*, **6**, 329–338.
40. Rain,J.C., Rafi,Z., Legrain,P. and Krämer,A. (1998) Conservation of functional domains involved in RNA binding and protein-protein interactions in human and *Saccharomyces cerevisiae* pre-mRNA splicing factor SF1. *RNA*, **4**, 551–565.
41. Rutz,B. and Seraphin,B. (1999) Transient interaction of BBP/ScF1 and Mud2 with the splicing machinery affects the kinetics of spliceosome assembly. *RNA*, **5**, 819–831.
42. Wang,Q., Zhang,L., Lynn,B. and Rymond,B.C. (2008) A BBP-Mud2p heterodimer mediates branchpoint recognition and influences splicing substrate abundance in budding yeast. *Nucleic Acids Res.*, **36**, 2787–2798.
43. Liu,Z., Luyten,I., Bottomley,M.J., Messias,A.C., Houngninou-Molango,S., Sprangers,R., Zanier,K., Krämer,A. and Sattler,M. (2001) Structural basis for recognition of the intron branch site RNA by splicing factor 1. *Science*, **294**, 1098–1102.
44. Wiesner,S., Stier,G., Sattler,M. and Macias,M.J. (2002) Solution structure and ligand recognition of the WW domain pair of the yeast splicing factor Prp40. *J. Mol. Biol.*, **324**, 807–822.
45. Zhang,Y., Madl,T., Bagdiul,I., Kern,T., Kang,H.S., Zou,P., Mäusbacher,N., Sieber,S.A., Krämer,A. and Sattler,M. (2013) Structure, phosphorylation and U2AF65 binding of the N-terminal domain of splicing factor 1 during 3′-splice site recognition. *Nucleic Acids Res.*, **41**, 1343–1354.
46. Wang,W., Maucuer,A., Gupta,A., Manceau,V., Thickman,K.R., Bauer,W.J., Kennedy,S.D., Wedekind,J.E., Green,M.R. and Kielkopf,C.L. (2013) Structure of phosphorylated SF1 bound to $U2AF^{65}$ in an essential splicing factor complex. *Structure*, **21**, 197–208.
47. Gasch,A., Wiesner,S., Martin-Malpartida,P., Ramirez-Espain,X., Ruiz,L. and Macias,M.J. (2006) The structure and Prp40 FF1 domain and its interaction with the crn-TPR1 motif of Clf1 gives a new insight into the binding mode of FF domains. *J. Biol. Chem.*, **281**, 356–364.
48. Bonet,R., Ruiz,L., Morales,B. and Macias,M.J. (2009) Solution structure of the fourth FF domain of yeast Prp40 splicing factor. *Proteins*, **77**, 1000–1003.
49. Görnemann,J., Barrandon,C., Hujer,K., Rutz,B., Rigaut,G., Kotovic,K.M., Faux,C., Neugebauer,K.M. and Séraphin,B. (2011) Cotranscriptional spliceosome assembly and splicing are independent of the Prp40p WW domain. *RNA*, **17**, 2119–2129.
50. Bodenmiller,B., Wanka,S., Kraft,C., Urban,J., Campbell,D., Pedrioli,P.G., Gerrits,B., Picotti,P., Lam,H., Vitek,O. *et al.* (2010) Phosphoproteomic analysis reveals interconnected system-wide responses to perturbations of kinases and phosphatases in yeast. *Sci. Signal.*, **3**, rs4.
51. Strauss,E.J. and Guthrie,C. (1994) PRP28, a DEAD-box protein, is required for the first step of mRNA splicing *in vitro*. *Nucleic Acids Res.*, **22**, 3187–3193.
52. Chang,T.H., Latus,L.J., Liu,Z. and Abbott,J.M. (1997) Genetic interactions of conserved regions in the DEAD-box protein Prp28p. *Nucleic Acids Res.*, **24**, 5033–5040.
53. Förch,P., Puig,O., Kedersha,N., Martínez,C., Granneman,S., Séraphin,B., Anderson,P. and Valcárcel,J. (2000) The aopoptosis-promoting factor TIA-1 is a regulator of alternative pre-mRNA splicing. *Mol. Cell*, **6**, 1089–1098.
54. Gabut,M., Chaudry,S. and Blencowe,B.J. (2008) The splicing regulatory machinery. *Cell*, **133**, 192.
55. Roca,X., Krainer,A.R. and Eperon,I.C. (2013) Pick one, but be quick: 5′ splice sites and the problems of too many choices. *Genes Dev.*, **27**, 129–144.
56. Parker,R., Siliciano,P.G. and Guthrie,C. (1987) Recognition of the TACTAAC box during mRNA splicing in yeast involves base pairing to the U2-like snRNA. *Cell*, **49**, 229–239.
57. Smith,D.J., Konarska,M.M. and Query,C.C. (2009) Insights into branch nucleophile positioning and activation from an orthogonal pre-mRNA splicing system in yeast. *Mol. Cell*, **34**, 333–343.
58. Perriman,R. and Ares,M. (2010) Invariant U2 snRNA nucleotide from a stem loop to recognize the intron early in splicing. *Mol. Cell*, **38**, 416–427.
59. Selenko,P., Gregorovic,G., Sprangers,R., Stier,G., Rhani,Z., Krämer,A. and Sattler,M. (2003) Structural basis for the molecular recognition between human splicing factors U2AF65 and SF1/BBP. *Mol. Cell*, **11**, 965–976.